ChemComm

COMMUNICATION

View Article Online
View Journal | View Issue

Cite this: *Chem. Commun.*, 2016, 52, 4926

Received 13th February 2016,
Accepted 4th March 2016

DOI: 10.1039/c6cc01352j

www.rsc.org/chemcomm

Biphenyl end-capped bithiazole co-oligomers for high performance organic thin film field effect transistors†

Kazuaki Oniwa,[a] Hiromasa Kikuchi,[a] Thangavel Kanagasekaran,[a] Hidekazu Shimotani,[b] Susumu Ikeda,[a] Naoki Asao,[a] Yoshinori Yamamoto,[ac] Katsumi Tanigaki[ab] and Tienan Jin*[a]

Two new regiospecific biphenyl end-capped bithiazole co-oligomers, BP2Tz(in) and BP2Tz(out), have been synthesized for application in thin film field effect transistors (TFTs). BP2Tz(in) with a 2,2′-bithiazole central unit exhibits a field effect hole mobility as high as 3.5 $cm^2 V^{-1} s^{-1}$. Green light emission is demonstrated for highly balanced ambipoar TFTs based on both BP2Tz(in) and BP2Tz(out).

The introduction of thiazole units having electron-accepting properties to π-conjugated backbones is one of the promising strategies in the design of high performance organic semiconducting materials, which is anticipated to lower the highest occupied molecular orbital (HOMO) and the lowest unoccupied molecular orbital (LUMO) energies and enhance the intermolecular interaction *via* the large polarity of thiazole rings.[1] In particular, since Katz *et al.* reported the first example of bithiazole-based oligothiophenes in organic thin film field effect transistors (OTFTs) in 1999,[2] a variety of thiazole-based semiconducting small molecules and polymers have been synthesized for application in high performance p- or n-channel OTFT devices.[3,4] For example, Yamashita *et al.* reported that the 5,5′-bithiazole-based oligomer with two electron-withdrawing 4-trifluoromethylphenyl end groups showed a high electron mobility of 1.83 $cm^2 V^{-1} s^{-1}$ in OTFT devices due to the lower LUMO energy and the strongly packed columnar structure with coplanar molecules, while in sharp contrast, the 2,2′-bithiazole-based analogous oligomer did not exhibit field effect transistor (FET) properties.[3a] Thiazole-based semiconductors without additional electron-withdrawing groups generally exhibit a p-type FET characteristic with improved oxidation stability compared to the oligo- and polythiophene analogues due to the down-shifted HOMO energies.[1] However, the large energy barrier between the lower HOMO energies and the work function of the Au electrodes results in less efficient charge injection. To date, the highest hole mobility of 0.33 $cm^2 V^{-1} s^{-1}$ has been achieved in the OFET device composed of a bithiazole-quaterthiophene copolymer.[4d]

On the other hand, a new class of biphenyl end-capped oligothiophenes,[5] for example, α,ω-bis(biphenylyl)terthiophene (BP3T) was found to be effective for high performance ambipolar organic light emitting FETs (OLETs).[6] OLETs combining both electroluminescence and FET functions have potential applications in active matrix displays and electrically driven organic lasers, and require materials to exhibit both high carrier mobility and high photoluminescence quantum yields (PLQYs).[7] Recently, we have demonstrated that the biphenyl end-capped bithiophene (BP2T)[8] and thienofuran (BPFT)[9] co-oligomers are promising OLET materials, exhibiting highly balanced ambipolar characteristics, good PLQYs, and light emission behavior in OFET devices.

Taking into consideration the profound properties of thiazole and biphenyl moieties, herein, we report a new class of regiospecific biphenyl end-capped bithiazole co-oligomers (BP2Tz), 5,5′-di([1,1′-biphenyl]-4-yl)-2,2′-bithiazole (**BP2Tz(in)**) and 2,2′-di([1,1′-biphenyl]-4-yl)-5,5′-bithiazole (**BP2Tz(out)**), including the synthesis, characterization, and OTFT device performance. OTFT devices composed of **BP2Tz(in)** showed a high hole mobility of 3.5 $cm^2 V^{-1} s^{-1}$, which is much higher than the previously reported thiazole-based semiconductors. Notably, green light emission was observed for highly balanced ambipolar TFT devices based on BP2Tz.

The synthetic method of BP2Tz is shown in Scheme 1. **BP2Tz(in)** was synthesized through a Pd-catalyzed homo-coupling of 2-bromothiazole and dibromination of the 5,5′-positions of the resulting 2,2′-bithiazole, followed by the double Suzuki–Miyaura coupling of the resulting 5,5′-dibromo-2,2′-bithiazole with [1,1′-biphenyl]-4-ylboronic acid. **BP2Tz(out)** was synthesized through the Suzuki–Miyaura coupling of 2-bromothiazole with [1,1′-biphenyl]-4-ylboronic acid followed by a selective organozinc-mediated homo-coupling of the resulting 2-([1,1′-biphenyl]-4-yl)thiazole.[10] Because of the poor solubility in organic solvents, **BP2Tz(in)** and **BP2Tz(out)** were purified by

[a] *WPI-Advanced Institute for Materials Research (WPI-AIMR), Tohoku University, Sendai 980-8577, Japan. E-mail: tjin@m.tohoku.ac.jp; Fax: +81-22-217-5979; Tel: +81-22-217-6177*

[b] *Graduate School of Science, Department of Physics, Tohoku University, Sendai 980-8578, Japan*

[c] *State Key Laboratory of Fine Chemicals, Dalian University of Technology, Dalian 116012, China*

† Electronic supplementary information (ESI) available. See DOI: 10.1039/c6cc01352j

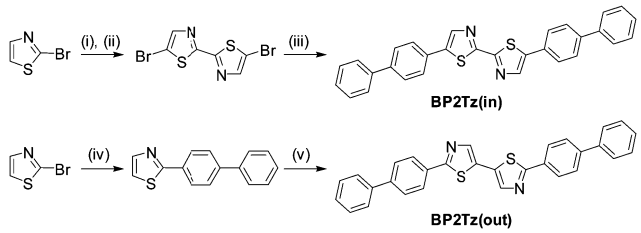

Scheme 1 Synthesis of BP2Tz co-oligomers. **BP2Tz(in)**: (i) $Pd(OAc)_2$ (10 mol%), n-Bu_4NBr (0.5 equiv.), DIPEA (1 equiv.), toluene, 105 °C, 48 h, 90%. (ii) NBS (4 equiv.), DMF, 60 °C, 95%. (iii) [1,1′-biphenyl]-4-ylboronic acid (2.5 equiv.), $Pd_2(dba)_3{\cdot}CHCl_3$ (5 mol%), X-phos, DMF, K_3PO_4, 120 °C, 40%. **BP2Tz(out)**: (iv) [1,1′-biphenyl]-4-ylboronic acid (1.2 equiv.), $Pd(PPh_3)_4$ (4 mol%), DMF, K_3PO_4, 100 °C, 70%. (v) $(TMP)_2Zn{\cdot}2MgCl_2{\cdot}2LiCl$, chloranil, THF, −40 °C to 0 °C, 12 h, 72%. DIPEA: diisopropylethyl amine, NBS: *N*-bromosuccinimide, DMF: dimethylformamide, TMP: 2,2,6,6-tetramethylpiperidinyl.

thermal sublimation. The structures of the BP2Tz were confirmed by elemental analysis.

The thermal properties of BP2Tz were evaluated by differential scanning calorimetry (DSC) and thermogravimetric analysis (TGA) (ESI,† Fig. S1). **BP2Tz(in)** and **BP2Tz(out)** showed lower melting points of 336 and 318 °C, respectively, compared to the bithiophene-biphenyl oligomer BP2T (370 °C).[1b,9] The TGA revealed that there was 10% weight loss at 447 and 432 °C for **BP2Tz(in)** and **BP2Tz(out)**, respectively, indicating their high thermal stability. It is noted that **BP2Tz(out)** exhibits two peaks at 318 and 336 °C in the DSC, which have been suggested to correspond to the metastable and stable crystalline phases by considering the X-ray diffraction (XRD) analyses of the **BP2Tz(out)** thin films deposited under various substrate temperatures (*vide infra*).

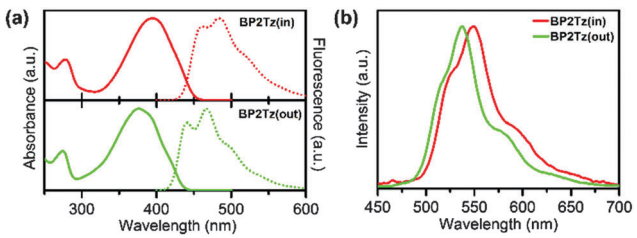

Fig. 1 Optical properties of BP2Tz. (a) UV-vis absorption and fluorescence spectra in $CHCl_3$ and (b) photoluminescence spectra in the solid state.

The optoelectronic properties of BP2Tz in chloroform and in the solid state are shown in Fig. 1 and Table 1. The absorption (λ_{abs}) and fluorescence (λ_{em}) maxima of **BP2Tz(in)** (394 nm and 461 nm) in solution are red-shifted compared to those of **BP2Tz(out)** (377 nm and 441 nm), indicating the narrow HOMO–LUMO band gap of the former. The fluorescence wavelengths of BP2Tz in the solid state significantly are red-shifted by about 90 nm as compared to those in solution and the absolute PLQYs (Φ_{PL}) of BP2Tz in the solid state (15% and 18%) are lower than that in solution (33%), indicating the strong intermolecular interaction of BP2Tz in the solid state. The optical band gaps are estimated from the absorption and fluorescence spectra in solution to be 2.81 eV for **BP2Tz(in)** and 2.92 eV for **BP2Tz(out)**, which are in consistency with the trend derived from density functional theory (DFT) calculations at the B3LYP/6-31G++** level (ESI,† Fig. S3). The HOMO energy levels of **BP2Tz(in)** (−5.49 eV) and **BP2Tz(out)** (−5.43 eV) deduced from photoelectron yield spectroscopy (PYS) are stabilized by introducing thiazole moieties (ESI,† Fig. S2).

The bottom-gate/top-contact OTFTs were fabricated *via* vacuum deposition of BP2Tz on the octadecyltrichlorosilane (OTS)-treated SiO_2/Si substrate at various substrate temperatures (T_{sub}) in the range of 40–180 °C during the deposition using gold as source and drain electrodes. The TFTs based on BP2Tz exhibit typical p-type FET characteristics and the T_{sub} dependent average hole mobility is shown in Fig. 2 (details in Table S3, ESI†). It is clear that the TFTs composed of **BP2Tz(in)** showed higher mobilities by at least one order of magnitude at various T_{sub}'s compared to those composed of **BP2Tz(out)**. The average mobilities of BP2Tz devices increased as T_{sub} was increased from 40 °C to 100 °C and decreased significantly at the T_{sub} value of 180 °C. The highest average mobility in the **BP2Tz(in)** device was observed as 3.2 $cm^2\ V^{-1}\ s^{-1}$ at the T_{sub} value of 100 °C with a threshold voltage (V_{th}) of −28 V and a very high current on/off ratio (I_{on}/I_{off}) of 10^8 (Table 1 and Fig. 3). It was noted that the best hole mobility of the **BP2Tz(in)** TFT was as high as 3.5 $cm^2\ V^{-1}\ s^{-1}$ at the T_{sub} value of 100 °C. The **BP2Tz(out)** TFT showed good performance for T_{sub} ranged from 100 to 160 °C with the highest average hole mobility of 0.4 $cm^2\ V^{-1}\ s^{-1}$ and I_{on}/I_{off} of 10^5 at the T_{sub} value of 100 °C.

The out-of-plane XRD patterns of the BP2Tz thin films deposited on the OTS-treated substrates at various T_{sub} were investigated to study the crystallinity of thin films with respect

Table 1 Summarized optoelectronic properties and OTFT performances using OTS/SiO_2/Si substrates

	$CHCl_3$ solution			Solid state					OTFTs[g]		
BP2Tz	λ_{abs} (nm)	λ_{em}[a] (nm)	Φ_f[b] (%)	λ_{em}[c] (nm)	Φ_{PL}[b] (%)	IP[d] (eV)	LUMO[e] (eV)	ΔE^{opt}[f] (eV)	μ_h ($cm^2\ V^{-1}\ s^{-1}$)	V_{th} (V)	I_{on}/I_{off}
BP2Tz(in)	394	461	33	550	15	5.49	−2.68	2.81	3.2	−28	10^8
BP2Tz(out)	377	441	33	537	18	5.43	−2.51	2.92	0.4	−19	10^5

[a] Excitation wavelengths: 394 nm for **BP2Tz(in)**, 377 nm for **BP2Tz(out)**. [b] Absolute quantum yield was determined by an integrating sphere system. Φ_f: fluorescence photoluminescence quantum yield. Φ_{PL}: photoluminescence quantum yield. [c] Excitation wavelength: 430 nm for **BP2Tz(in)**, 410 nm for **BP2Tz(out)**. [d] Ionization potential (IP) of thin film on the OTS-treated SiO_2 substrate was determined by using the photoemission yield spectrometer (Riken Keiki, AC-3). [e] LUMO was calculated from the IP values and the optical bandgap. [f] Optical bandgap (ΔE^{opt}) was estimated from the contact between the UV-vis absorption and the fluorescence spectra. [g] Au was used as source and drain electrodes, and average hole mobilities at the T_{sub} value of 100 °C are shown. OTFTs: organic thin film field effect transistors. T_{sub}: substrate temperature.

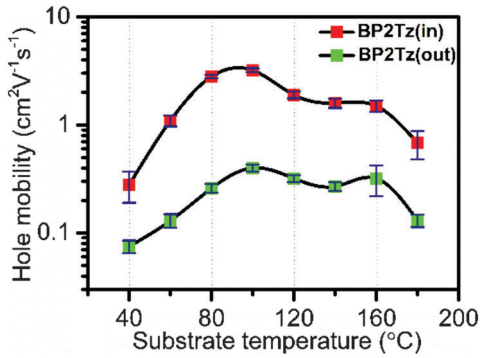

Fig. 2 Substrate temperature dependent average hole mobility of BP2Tz-TFTs.

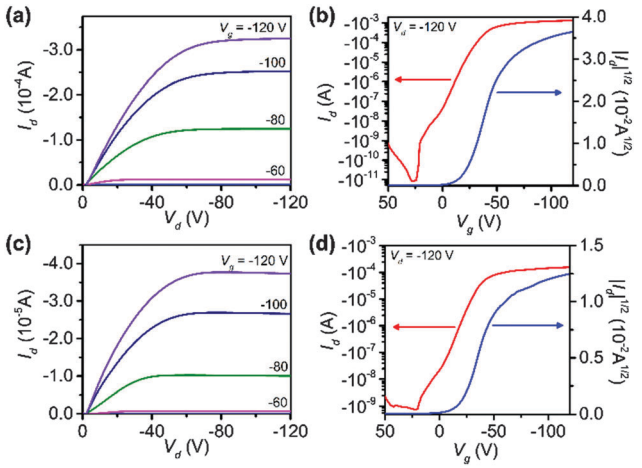

Fig. 3 Output (a) and transfer (b) characteristics of **BP2Tz(in)**-based OTFTs, output (c) and transfer (d) characteristics of **BP2Tz(out)**-based OTFTs at the T_{sub} value of 100 °C using OTS/SiO_2/Si substrates.

to the TFT performance (Fig. 4). The presence of a number of diffraction peaks in the higher angle region of the XRD patterns indicates the high film crystallinity of **BP2Tz(in)** and **BP2Tz(out)**. The (100) plane in the **BP2Tz(in)** XRD patterns corresponds to the *d*-spacing of 23.9 Å at the T_{sub} value of 40 °C which is shorter than the DFT calculated molecular length of 28.1 Å, indicating that the molecule stands on the substrate with a tilt angle of 58.3°. In addition, no change of the packing structure was found for the

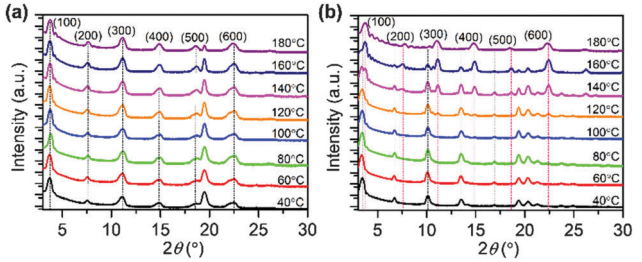

Fig. 4 X-ray diffraction patterns of BP2Tz thin films on the OTS-treated SiO_2/Si substrate at various substrate temperatures (T_{sub}). (a) **BP2Tz(in)**, (b) **BP2Tz(out)**.

BP2Tz(in) films at elevated T_{sub}'s. In sharp contrast, the **BP2Tz(out)** film at the T_{sub} value of 120 °C exhibits a new unrelated family of XRD patterns as compared to those of the thin films at 40–100 °C. The new peak intensity increases and the original peak intensity decreases upon further increasing the T_{sub} to 180 °C, suggesting the existence of the phase transition from the metastable to the stable crystalline phase in **BP2Tz(out)** films. The *d*-spacing of 25.9 Å calculated from the metastable film at the T_{sub} value of 40 °C indicates that the **BP2Tz(out)** molecule stands on the substrate with a tilt angle of 67.0° as estimated from the DFT calculated molecular length of 28.12 Å. On the other hand, the shorter *d*-spacing of 23.8 Å deduced from the new diffractions of the stable thin film at the T_{sub} value of 180 °C indicates that the molecule stands on the substrate with a tilt angle of 57.8°. The coexistence of the different packing structures within **BP2Tz(out)** films probably is one of the reasons for the reduced mobility.

The morphology of BP2Tz thin films deposited at various T_{sub} values was studied using scanning electron microscopy (SEM) (ESI,† Fig. S4 and S5). The amount of ribbon-like micro-crystals covering on the surfaces of BP2Tz thin films at lower T_{sub} diminished and the crystalline grains became large with the increasing T_{sub}. The **BP2Tz(out)** thin films showed more clear grain boundaries and rough morphological surfaces compared with the **BP2Tz(in)** thin films at T_{sub} ranging from 40 to 80 °C, implying the higher potential barriers between grains in the **BP2Tz(out)** films, which may reduce the charge transport efficiency.[11] At T_{sub} higher than 100 °C, the grain boundaries become almost invisible and terrace structures with smooth surfaces are observed, and therefore the higher mobility is obtained. However, the mobilities decreased significantly for the films at the T_{sub} value of 180 °C, in spite of their rather smooth surfaces, which is probably due to the cracked surfaces observed in these thin films.

By using tetratetracontane (TTC) as a passivation layer modified on a SiO_2/Si substrate instead of OTS, a highly balanced ambipolar charge transport characteristic was achieved for the TFTs composed of **BP2Tz(in)** or **BP2Tz(out)** thin films with balanced hole and electron mobilities of about 10^{-2} cm^2 V^{-1} s^{-1} (ESI,† Fig. S6 and S7). The TFT devices were fabricated *via* vacuum deposition of BP2Tz onto the TTC/SiO_2/Si substrate maintaining T_{sub} at room temperature followed by deposition of Au electrodes. We have demonstrated previously that the TTC surface modification layer has enhanced the gap states at the metal–semiconductor interface which will enhance the efficient electron injection from the Au electrode to the semiconducting layer.[8b] Notably, bright light emission was observed from both BP2Tz-TFT devices by applying gate voltages (V_g) from 0 to 160 V at a constant drain voltage (V_d) of 160 V (Fig. 5 and Fig. S8). The light emission zone was moved between the source and the drain electrodes by varying V_g at a fixed V_d. This light emission should be ascribed to the highly balanced ambipolar charge transport behavior and good photoluminescence efficiency of BP2Tz.

In conclusion, we have demonstrated that new regiospecific biphenyl end-capped bithiazole co-oligomers exhibited high OTFT performances. **BP2Tz(in)** with unique crystallinity and smooth thin film morphology showed a field effect hole mobility

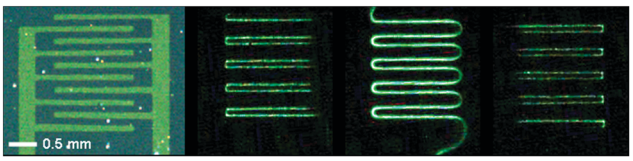

Fig. 5 Light emission of an ambipolar OTFT based on **BP2Tz(in)**.

as high as 3.5 $cm^2 V^{-1} s^{-1}$ and an on/off ratio 10^8 at the optimal T_{sub} of 100 °C. Notably, green light emission was observed for ambipolar OTFT devices based on both **BP2Tz(in)** and **BP2Tz(out)** using the TTC/SiO_2/Si substrate. This observation may provide a promising strategy to develop new organic light emitting transistor materials possessing both high photoluminescence efficiency and charge mobility.

This work was supported by the Grants-in-Aid for Scientific Research (B) from the Japan Society for Promotion of Science (JSPS) (No. 25288043), and the World Premier International Research Center Initiative (WPI), MEXT, Japan. K. O. acknowledges the support of the JSPS Research Fellowships for Young Scientists.

Notes and references

1 (*a*) R. P. Ortiz, H. Yan, A. Facchetti and T. J. Marks, *Materials*, 2010, **3**, 1533; (*b*) Y. Lin, H. Fan, Y. Li and X. Zhan, *Adv. Mater.*, 2012, **24**, 3087; (*c*) C. Wang, H. Dong, W. Hu, Y. Liu and D. Zhu, *Chem. Rev.*, 2012, **112**, 2208.

2 W. Li, H. E. Katz, A. J. Lovinger and J. G. Laquindanum, *Chem. Mater.*, 1999, **11**, 458.

3 (*a*) S. Ando, R. Murakami, J.-I. Nishida, H. Tada, Y. Inoue, S. Tokito and Y. Yamashita, *J. Am. Chem. Soc.*, 2005, **127**, 14996; (*b*) M. Akhtaruzzaman, N. Kamata, J.-i. Nishida, S. Ando, H. Tada, M. Tomura and Y. Yamashita, *Chem. Commun.*, 2005, 3183; (*c*) M. Mamada, J.-I. Nishida, D. Kumaki, S. Tokito and Y. Yamashita, *Chem. Mater.*, 2007, **19**, 5404; (*d*) T. Kojima, J. Nishida, S. Tokito and Y. Yamashita, *Chem. Lett.*, 2007, **36**, 1198; (*e*) T. Kojima, J.-I. Nishida, S. Tokito, H. Tada and Y. Yamashita, *Chem. Commun.*, 2007, 1430; (*f*) M. Mamada, J.-I. Nishida, S. Tokito and Y. Yamashita, *Chem. Commun.*, 2009, 2177; (*g*) H. Usta, W. C. Sheets, M. Denti, G. Generali, R. Capelli, S. Lu, X. Yu, M. Muccini and A. Facchetti, *Chem. Mater.*, 2014, **26**, 6542.

4 (*a*) X. M. Hong, H. E. Katz, A. J. Lovinger, B.-C. Wang and K. Raghavachari, *Chem. Mater.*, 2001, **13**, 4686; (*b*) H. Moon, W. S. Jahng and M. D. Curtis, *J. Mater. Chem.*, 2008, **18**, 4856; (*c*) J. Liu, R. Zhang, I. Osaka, S. Mishra, A. E. Javier, D.-M. Smilgies, T. Kowalewski and R. D. McCullough, *Adv. Funct. Mater.*, 2009, **19**, 3427; (*d*) D. H. Kim, B.-L. Lee, H. Moon, H. M. Kang, E. J. Jeong, J.-I. Park, K.-M. Han, S. Lee, B. W. Yoo, B. W. Koo, J. Y. Kim, W. H. Lee, K. Cho, H. A. Becerril and Z. Bao, *J. Am. Chem. Soc.*, 2009, **131**, 6124; (*e*) I. H. Jung, J. Yu, E. Jeong, J. Kim, S. Kwon, H. Kong, K. Lee, H. Y. Woo and H.-K. Shim, *Chem. – Eur. J.*, 2010, **16**, 3743; (*f*) H. Kong, S. Cho, D. H. Lee, N. S. Cho, M.-J. Park, I. H. Jung, J.-H. Park, C. E. Park and H.-K. Shim, *J. Polym. Sci., Part A: Polym. Chem.*, 2011, **49**, 2886; (*g*) X. Guo, J. Quinn, Z. Chen, H. Usta, Y. Zheng, Y. Xia, J. W. Hennek, R. P. Ortiz, T. J. Marks and A. Facchetti, *J. Am. Chem. Soc.*, 2013, **135**, 1986; (*h*) M. Durso, D. Gentili, C. Bettini, A. Zanelli, M. Cavallini, F. D. Angelis, M. G. Lobello, V. Biondo, M. Muccini, R. Capellibe and M. Melucci, *Chem. Commun.*, 2013, **49**, 4298; (*i*) J. Lee, J. W. Chung, J. Jang, D. H. Kim, J.-I. Park, E. Lee, B.-L. Lee, J.-Y. Kim, J. Y. Jung, J. S. Park, B. Koo, Y. W. Jin and D. H. Kim, *Chem. Mater.*, 2013, **25**, 1927.

5 S. Hotta, T. Yamao, S. Z. Bisri, T. Takenobu and Y. Iwasa, *J. Mater. Chem. C*, 2014, **2**, 965.

6 S. Z. Bisri, T. Takenobu, Y. Yomogida, H. Shimotani, T. Yamao, S. Hotta and Y. Iwasa, *Adv. Funct. Mater.*, 2009, **19**, 1728.

7 (*a*) M. Muccini, *Nat. Mater.*, 2006, **5**, 605; (*b*) F. Cicoira and C. Santato, *Adv. Funct. Mater.*, 2007, **17**, 3421; (*c*) J. Zaumseil and H. Sirringhaus, *Chem. Rev.*, 2007, **107**, 1296.

8 (*a*) Y. Wang, R. Kumashiro, Z. Li, R. Nouchi and K. Tanigaki, *Appl. Phys. Lett.*, 2009, **95**, 103306; (*b*) T. Kanagasekaran, H. Shimotani, S. Ikeda, H. Shang, R. Kumashiro and K. Tanigaki, *Appl. Phys. Lett.*, 2015, **107**, 043304.

9 K. Oniwa, T. Kanagasekaran, T. Jin, M. Akhtaruzzaman, Y. Yamamoto, H. Tamura, I. Hamada, H. Shimotani, N. Asao, S. Ikeda and K. Tanigaki, *J. Mater. Chem. C*, 2013, **1**, 4163.

10 S. H. Wunderlich and P. Knochel, *Angew. Chem., Int. Ed.*, 2007, **46**, 7685.

11 A. D. Carlo, F. Piacenza, A. Bolognesi, B. Stadlober and H. Maresch, *Appl. Phys. Lett.*, 2005, **86**, 263501.